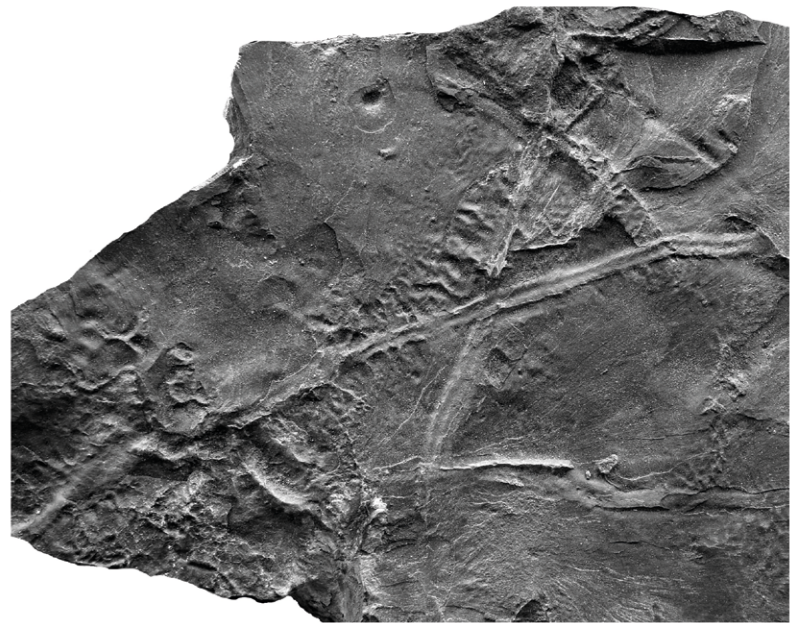


Ammonite stratigraphy and fossils of the Passwang Formation (Middle Jurassic) and the Opalinus Clay (Early to Middle Jurassic), excavated in Ga18 and the Niches P3, Passwang and CO₂ in the Mont Terri Rock Laboratory



Reports of the Swiss Geological Survey
Berichte der Landesgeologie
Rapports du Service géologique national
Rapporti del Servizio geologico nazionale

Bernhard Hostettler, Volker Dietze,
David Jaeggi, Ursula Menkveld-Gfeller,
Christophe Nussbaum & Paul Bossart



Schweizerische Eidgenossenschaft
Confédération suisse
Confederazione Svizzera
Confederaziun svizra

Swiss Confederation

Federal Office of Topography swisstopo
www.swisstopo.ch

Editor

Federal Office of Topography (swisstopo)

Authors

Bernhard Hostettler, Volker Dietze, David Jaeggi, Ursula Menkveld-Gfeller,
Christophe Nussbaum, Paul Bossart

Keywords

Middle Jurassic, Opalinus Clay, Passwang Formation, Sissach Member, ammonites,
biostratigraphy

Frontcover

Gyrochorte isp., NMBE 5035775. Ga18, Opalinus Clay, upper sandy facies

Copyright

© swisstopo, CH-3084 Wabern, 2021

pdf file available at www.swisstopo.ch

Ammonite stratigraphy and fossils of the Passwang Formation (Middle Jurassic) and the Opalinus Clay (Early to Middle Jurassic), excavated in Ga18 and the Niches P3, Passwang and CO₂ in the Mont Terri Rock Laboratory

Bernhard Hostettler¹, Volker Dietze², David Jaeggi³, Ursula Menkveld-Gfeller¹,
Christophe Nussbaum³ & Paul Bossart³

¹Naturhistorisches Museum Bern, Bernastrasse 15, 3005 Bern, Switzerland

²Meraner Strasse 41, 86720 Nördlingen, Germany

³Federal Office of Topography swisstopo, Seftigenstrasse 264, 3084 Wabern, Switzerland



Schweizerische Eidgenossenschaft
Confédération suisse
Confederazione Svizzera
Confederaziun svizra

Swiss Confederation

Federal Office of Topography swisstopo
www.swisstopo.ch

Table of contents

Summary	6
1. Introduction	7
1.1 Aims and objectives	7
1.2 Material and methods	7
1.3 Previous biostratigraphic investigations	8
2. Results	9
2.1 Lithology, fossils, and biostratigraphy of Ga18 and Niches P3, Passwang, and CO ₂	9
2.1.1 Niche CO ₂ : Lower shaly facies/ carbonate rich sandy facies	9
2.1.2 Ga18: Upper shaly facies	9
2.1.3 Ga18: Upper sandy facies.	9
2.1.4 Ga18: Boundary Opalinus Clay/ Passwang Formation (Sissach Member)	10
2.1.5 Description of the section Ga18/Niche P3 (Sissach Member and a lithostratigraphically not subdivided area of the Passwang Formation) (for section see Fig. 5)	13
2.1.6 Niche Passwang	17
2.2 Comparison with the BDB-1 drill core	18
3. Discussion	22
4. Conclusions	24
References	25
Acknowledgements	27

List of figures

Fig. 1:	Location of Gallery 18 (Ga18) and niches in the Rock Laboratory	8
Fig. 2:	Location of windows (F1–F17) and sections in a 3D view of the Ga18	8
Fig. 3:	Concretions with shrinkage cracks, upper sandy facies, Ga18 (NMBE 5035815)	10
Fig. 4:	Legend to the sections	11
Fig. 5:	Lithological section of the late Opalinus Clay and a part of the Passwang Formation in Ga 18/Niche P3 (modified after HOSTETTLER et al. 2020)	12
Fig. 6:	Sample from Layer 28, the base of the Passwang Formation with limonitic intraclasts (NMBE 5035816)	13
Fig. 7:	Rock sample with <i>Zoophycos</i> isp. MASSALONGO 1855 (NMBE 5035817)	14
Fig. 8:	Flat, stromatolitic iron-hydroxide crusts in Layer 30 (NMBE 5035818)	14
Fig. 9:	Silty claystone with light grey to light bluish grey sandy lenses, rock sample from Layer 49a (NMBE 5035819)	17
Fig. 10:	Lithological section through the Passwang Formation in Niche Passwang compared to the section of Ga18/Niche P3. Legend: * in the section of Niche Passwang = lower part of the Sissach Member	19
Fig. 11:	Possible lithostratigraphic correlation of the sections Sous les Roches, Ga18/Niche P3 (Mont Terri Rock Laboratory) and BDB-1 well (Mont Terri Rock Laboratory).	21

List of tables

Table 1:	Comparison of the results of the ammonite stratigraphy of the Opalinus Clay, the Sissach Member and the overlying lowermost iron-oid bearing part of the Passwang Formation of the BDB-1 well (not subdivided in the study area) with those of Ga18/Niche P3	20
----------	--	----

Appendix

Plates I–V	30–39
Description of the geological windows (F1–F17)	40–41

Summary

During the construction of the new gallery Ga18 at the Mont Terri Rock Laboratory, we recorded two lithostratigraphic sections through the Sissach Member of the Passwang Formation and examined the excavated material for macrofossils. Compared to previous investigations, we could significantly improve our knowledge of the fossils in individual layers and the ammonite stratigraphy. With the exception of the Murchisonae Subzone, we could date all ammonite Zones and Subzones of the period from Early Aalenian to Early Bajocian (Middle Jurassic). In addition, the new profile surveys also allowed us to make a better regional correlation of the lithostratigraphic units studied here. We find that the thickness of the sequence Sissach Member to the probably Hirnichopf Member of the Passwang Formation increases rapidly from the southern edge of the Delémont Basin to the Mont Terri Rock Laboratory.

1. Introduction

Biostratigraphic investigations have already been carried out in the Mont Terri Rock Laboratory in the past. In the earliest study, REISDORF et al. (2014) investigated rock material from a freshly excavated niche (i.e., window). Biostratigraphic dating was done with ammonites and ostracods. It was found that a considerable part of the Opalinus Clay belongs to the Late Toarcian, contrary to expectations. Subsequently, REISDORF et al. (2016) and HOSTETTLER et al. (2017) examined biostratigraphically the 250 m-long, cored BDB-1 well that, in the Rock Laboratory, penetrated the surrounding rocks of the Passwang and parts of the Staffelegg Formations as well as the entire Opalinus Clay. These authors dated the BDB-1 drillcore with palynomorphs, ostracods, and ammonites.

1.1 Aims and objectives

The aim of the present work is to obtain a higher resolution ammonite stratigraphy, especially in the Passwang Formation, by means of fossil collections that were collected bed-by-bed as precisely as possible. In addition, we wanted to record, as detailed as possible, two lithological sections (Ga18/Niche P3 and Niche Passwang) in the Passwang Formation. We also decided to include an investigation of the Opalinus Clay excavated in Ga18. Here, however, we were forced to waive recording one section due to safety considerations. For the entire geological documentation of Ga18 including 220 daily mappings, geological and structural maps carried out by the operator swisstopo, please refer to JAEGGI et al. (2020).

1.2 Material and methods

The tunnel of Gallery 18 (Ga18, (see Figs. 1 and 2) was excavated with a relatively small 35 t road header. This machine produced rock fragments of only a few cm to a few dm in diameter, hindering recovery of complete fossil material of larger size. In particular, large objects were often heavily damaged. Fossil recovery was not possible in the gallery or the niches, on the one hand due to lack of time (in Ga18 mapping time was normally limited to 30 min, half of which was used to document the excavation). On the other hand, hardness of the rock did not permit us to remove fossils easily. The material was therefore collected from the tailings temporarily stored in the halls of the former St-Ursanne lime factory. The fossils were collected in the time interval from March 2018 to August 2019. Collection of the fossil material usually took place during or after excavation. If this was not possible, the stored piles were marked with the date of excavation and examined later. The characteristic lithologies could usually be correlated with the different layers in the Ga18 during measuring of the sections without any problem, so that a more-or-less bed-by-bed collection was possible. Only Layers 33–37 (with the exception of Layer 35) and Layers 40–42 could not be identified by lithology from the excavation piles with cer-

tainty. Thus, these are summarized in the classification of finds as Layers 33–37 and Layers 40–42.

Fossils were prepared mechanically (compressed air tool, sandblaster) and chemically (potassium hydroxide, formic acid). All macrofossils found and described in the frame of the present study are kept in the collection of the Natural History Museum of Bern (NMBE).

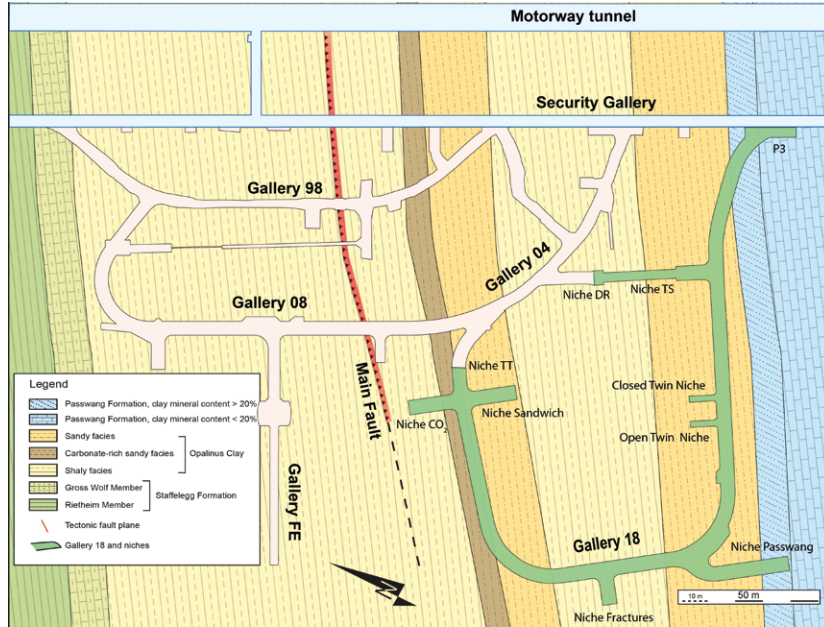


Figure 1: Location of Gallery 18 (Ga18) und niches in the Rock Laboratory.

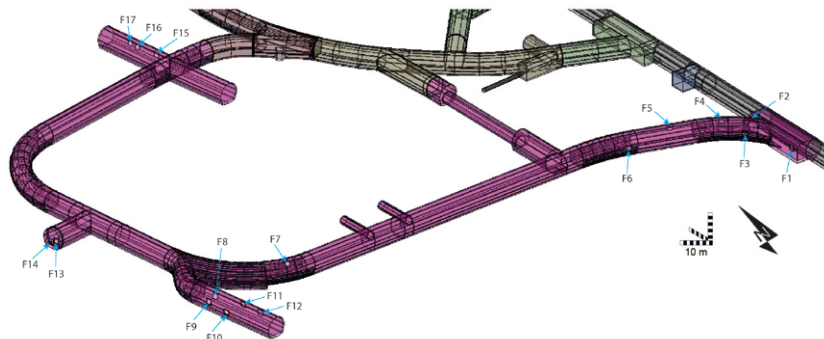


Figure 2: Location of windows (F1–F17) and sections in a 3D view of the Ga18.

1.3 Previous biostratigraphic investigations

The earliest study was conducted in 2014 (REISDORF et al. 2014) where the Opalinus Clay was dated using the windows available in the Rock Laboratory and the excavation material from the FE niche (see Fig. 1). Surprisingly, a section approximately 30 m thick appeared to belong to the Toarcian rather than to the Aalenian as originally assumed.

A more detailed survey and investigation of the 250 m-long drillhole BDB-1 (REISDORF et al. 2016 and HOSTETTLER et al. 2017) confirmed this result. In addition, these studies described and dated the underlying and overlying rocks of the Stafflegg Formation and the Passwang Formation.

2. Results

2.1 Lithology, fossils, and biostratigraphy of Ga18 and Niches P3, Passwang, and CO₂

2.1.1 Niche CO₂: Lower shaly facies/carbonate rich sandy facies

Niche CO₂ is located completely within the Opalinus Clay (see Fig. 1). The lowermost part reaches into the lower shaly facies. Some layers in these excavated argillaceous rocks were rich in fossils: *Bositra buchi* (ROEMER, 1836) (see also Plate I, Figs. 4a, b) was the most common. Other bivalves are *Palaeonucula hammeri* (DEFRANCE 1825) (Plate I, Fig. 7) and *Nuculana claviformis* (SOWERBY 1824) (Plate I, Fig. 9). Some gastropods could be assigned to the species *Amphitrochus subduplicatus* var. *palinurus* (D'ORBIGNY 1850) (Plate I, Fig. 8). The figured ammonites belong to *Leioceras subglabrum* (BUCKMAN, 1902) (Plate 1, Figs. 1, 2, 3 top right) and *Cylicoceras* sp. (Plate 1, Fig. 3 left bottom), both typical for the oldest Opalinum Subzone (CONTINI et al. 1997). These ammonites were found in different preservations. Apart from flattened internal moulds, which sometimes still show remains of the periostracum, completely compressed specimens with shell preservation (recrystallized calcite) are common. The specimens with three-dimensional preserved body chamber (Plate 1, Fig. 2) are conspicuous. In these specimens, the body chamber is mostly preserved as internal mould and the phragmocone is completely flattened and is preserved with recrystallized shell.

In the carbonate-rich sandy facies, we found one sample containing numerous small oysters (see also Plate I, Fig. 11/2). In addition to some echinid spines (Plate I, Fig. 10), crinoid skeletal elements are also present. For the first time, a small ammonite (Plate I, Fig. 5), probably belonging to the genus *Leioceras*, was found. On the surface of the layers there are indeterminate burrow traces (not figured).

2.1.2 Ga18: Upper shaly facies

Fossils in the upper shaly facies proved to be very sparse. In small nests, *Bositra buchi* (ROEMER 1836) (see also plate I, Figs. 4a, b) could be found. The trace fossil *Gyrochorte* HEER 1865 was also found in some thin sandy layers (see also Plate II, Fig. 1).

2.1.3 Ga18: Upper sandy facies

The upper sandy facies comprises claystone interspersed with thin layers and lenses of silt and sand. For the first time some fossils could be recovered from this strata. Frequent are trace fossils (Plate II, Fig. 1) that can be assigned to the Ichnotaxon *Gyrochorte* HEER 1865. *Bositra buchi*

(ROEMER 1836) also occurs in small lenses and in thin layers (see also Plate I, Figs. 4a, b). Interesting are some ammonites and ammonite fragments. These we tentatively assigned to the species *Leioceras* ex gr. *opalinum* (REINECKE 1818) (Plate I, Fig. 12). In some thin lenses or layers we found accumulations of calcitic shells of bivalves, especially oysters (Plate I, Fig. 11/2), and skeletal remains of the crinoid *Chariocrinus wuerttembergicus* (OPPEL 1856) (Plate I, Fig. 11/1). Rarely we found ossicles of an unidentified starfish and remains of a cidaroid sea urchin (plate I, Fig. 11/3). The carbonate-rich layers are enriched in small fossils and fossil fragments. In addition, there are large concretions with shrinkage cracks (see Fig. 3). These are mostly filled with calcite crystals. Sometimes these concretions also include shell accumulations. Some three-dimensional remains of ammonites, for example, are preserved in these layers.

2.1.4 Ga18: Boundary Opalinus Clay/Passwang Formation (Sissach Member)

At the Rock Laboratory, the Opalinus Clay/Sissach Member boundary has been defined using the drillcore of the BDB-1 well. Excavation of Ga18 made it possible to view this for the first time within a larger sample volume. At the base of Layer 28 (see Figs. 4 and 5), which marks the base of the Passwang Formation (definition sensu REISDORF et al. 2016, HOSTETTLER et al. 2017), there is often an accumulation of crinoid skeletal elements.



Figure 3: Concretions with shrinkage cracks, upper sandy facies, Ga18 (NMBE 5035815).

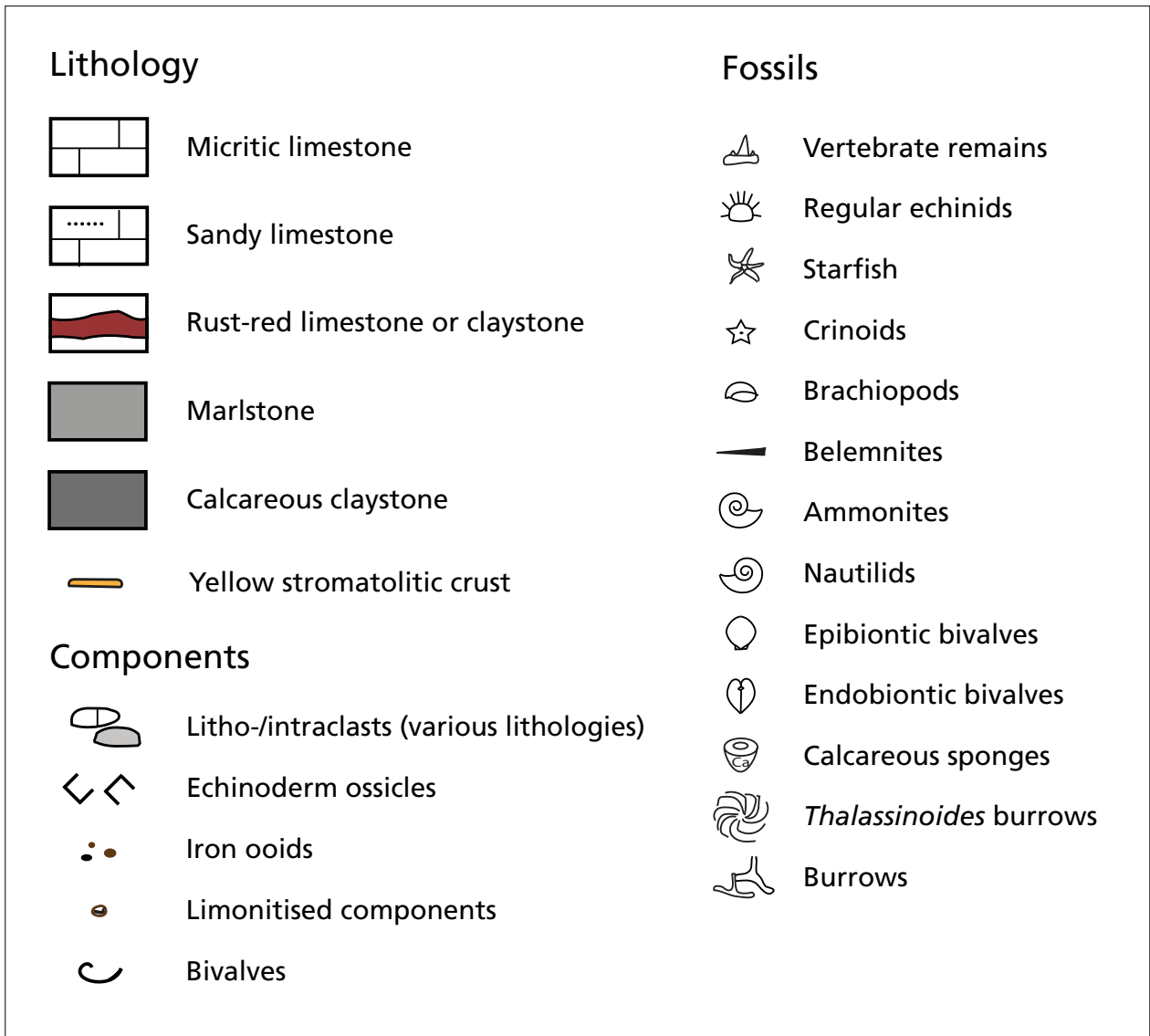


Figure 4: Legend to the sections.

Layer 27 is a dark grey claystone with thin silty layers and lenses and indeterminate burrows.

Layer 28 consists of an argillaceous limestone with echinoderm skeletal remains and chamositic iron ooids in the matrix. It contains mostly rounded, but also flattened, litho- and intraclasts. Some of these clasts measure more than 10 cm in diameter and are covered with thin stromatolitic crusts (see Fig. 6). A larger clast shows additional serpulid growth. The clasts consist mostly of argillaceous limestone, sometimes also of light brown to grey iron-oolitic material. The iron-oolitic clasts contain echinoderm skeletal remains and shell fragments.



Figure 6: Sample from Layer 28, the base of the Passwang Formation, with limonitic intraclasts (NMBE 5035816).

Some of the clasts exhibit small borings. In the upper part of the layer, the clasts are embedded in a clay matrix. Two of them appear to be fragments of body chambers of *Leioceras* sp. However, they are so strongly abraded that an unambiguous classification is not possible. A small Rhychonellid species could be found in the limy, iron-oid bearing area. Fossils are more frequent in the silvery, dark grey marl directly above the boundary horizon.

2.1.5 Description of the section Ga18/Niche P3 (Sissach Member and a lithostratigraphically not subdivided area of the Passwang Formation) (for section see Fig. 5)

Layer 29a: this dark grey marl begins at the hangingwall of Layer 28. It contains bivalves and, more rarely, ammonites. A *Leioceras* ex gr. "*comptum*" (Plate II, Fig. 2) could be recovered, indicating the "Comptum" Subzone, Opalinus Zone. Epibiontic bivalves such as *Chlamys textoria* (SCHLOTHEIM 1820) are also common (see also Plate V, Fig. 4). Above it follows an approx. 3.5 m thick, light grey sandy marl succession with sandy limestone concretions and layers (Layer 29b). This layer is strongly biotur-

bated. In some layers the ichnotaxon *Zoophycos* isp. MASSALONGO 1855 (Fig. 7) is very common.

Apart from bivalves and bivalve fragments, no macrofossils were found here.

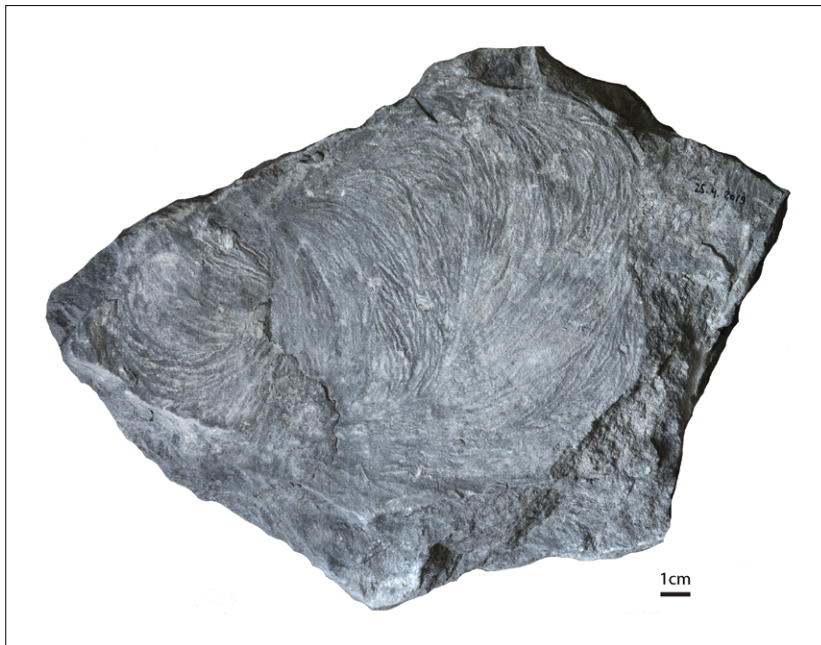


Figure 7: Rock sample with *Zoophycos* isp. MASSALONGO 1855 (NMBE 5035817).

Layer 30 is a brown biotrititic marl. Locally, ochre-coloured flat stromatolitic iron-hydroxide crusts are typical. These exhibit thicknesses of less than one cm but sometimes reach almost the size of the palm of a hand (Fig. 8). Layer 30 contains numerous echinoderm skeletal fragments. Frequent are spines of *Caenocidaris royssii* (DESOR 1858) (Plate II, Figs. 5, 6). Some of them are abraded, with borings, or incomplete. Occasional small spherical bryozoic colonies occur. We found fragments of shells, rare calcareous sponges and also the fragment of a shark tooth, which can be most likely assigned to the genus *Asteracanthus*.



Figure 8: Flat, stromatolitic iron-hydroxide crusts in Layer 30 (NMBE 5035818).

Layer 31 is a grey biodetritus-bearing sandy limestone. In addition to the primary spines of *Caenocidaris royssii*, bivalves of the genus *Entolium* (Plate III, Fig. 5) are common. Other bivalves such as *Gresslya* sp. and *Pholadomya* sp. (Plate II, Fig. 8) also occur in this layer. We assigned the ammonites found here provisionally to the genus *Ancolioceras* nov. sp. (Plate II, Figs. 3, 4), since the keel of the only specimen preserved with a complete body chamber extends, in an attenuated fashion, to the aperture. We assign these forms of *Ancolioceras* sp. to a group that so far is only known from Geisingen (SW Germany) (DIETZE et al. 2014). This group is still unnamed. Their biostratigraphic classification lies at the boundary of the “Comptum” Subzone (Opalinum Zone) and the Haugi Subzone (Murchisonae Zone).

Layer 32 is a greenish grey biodetritic marl with limonitised components. Very frequent are unidentified echinid remains and primary spines of *Caenocidaris royssii* (DESOR 1858) (see also Plate II, Figs. 5, 6). In this layer we also found the only fragment of the test of this species (Plate II, Fig. 7). It consists of about two interambulacra with the intervening ambulacrum.

Layer 33 is a grey biodetritus bearing, sandy limestone. The only ammonite found in this layer is *Ludwigia crassa* HORN 1909 (Plate III, Fig. 1). This can biostratigraphically be placed in the Haugi Subzone of the Murchisonae Zone. The bivalve *Pholadomya fidicula* (SOWERBY 1826) (Plate III, Fig. 9) and the belemnite *Brevibelus breviformis* (VOLTZ 1830) (Plate III, Fig. 2) also occur.

Layers 34, 36–37: Succession of grey sandy biodetritus-bearing limestones. A plesiosaur vertebra is shown in Plate II, Figs. 9a, b.

Layer 35: Dark grey sandy marls. The bivalve *Goniomya literata* (SOWERBY 1819) originate from this layer (Plate III, Fig. 4).

From **Layer 38** come two incomplete sea urchin spines, which might belong to the genus *Diplocidaris* (Plate III, Fig. 6). Lithology: Dark grey sandy marls. Note: VADET (1991) assigned identical spines from Böttstein (Aargau) to the species *Laurenticidaris impar* (DUMORTIER 1875). New finds of the same type of spines and corona fragments from the Böttstein locality can now be clearly identified as belonging to the genus *Diplocidaris*.

Layer 39: Ammonites are occasionally found in this grey limestones, including an *Ancolioceras* sp. (Plate III, Fig. 3), indicating Murchisonae Zone, Haugi Subzone. In addition, unidentified small bivalves (Plate III, Fig. 8) are frequent.

Layers 40–42 comprise grey, fossil-poor limestones.

Layer 43 is a dark grey fossil-poor marlstone.

Layer 44 is a grey-brown to yellow-brown biodetritus-bearing iron oolite. It often exhibits vertical, greenish-coloured burrows. The biodetritus consists of echinoderm skeletal remnants. Bivalves are also quite common. The only ammonite originating from this layer (Plate III, Fig. 10) belongs to the genus *Brasilia* and can be assigned to the Bradfordensis Zone and Subzone.

Layer 45 is of the same lithology as the Layer 44 but red coloured.

Layer 46a is a grey to brown, somewhat inhomogeneous biotrititic limestone with small iron ooids and limonitised components. There are also grey to rust-brown intraclasts of an argillaceous limestone locally measuring several cm. These clasts contain mostly biotrititus. In larger clasts there are also traces of burrows. The recrystallized shells of the fossils are partially strongly dissolved. This layer is generally rich in fossils, most common are ammonites. Among these are different species of the genus *Brasilia* (Plate IV, Fig. 1–4 and Plate V, Fig. 11). More rare are bivalves, such as *Ctenostreon* sp. (Plate V, Fig. 9) and *Oxytoma inaequivalvis* (SOWERBY 1819) (not figured), and belemnites. A large terebratulid (Plate III, Fig. 7) belongs to the species *Gigantothyris* cf. *gigantea* SEIFERT 1963. This terebratulid seems to occur quite frequently in the Gigantea Subzone, for instance, at Grangiéron JU, or at Hirnichopf (Passwang, SO).

Layer 46b consists of grey, somewhat argillaceous limestone with iron ooids, often chamositic. Echinoderm skeletal elements are locally common. Also conspicuous are small, ochre-coloured, iron-oolithic intraclasts. The ammonites (Plate IV, Figs. 5–7; Plate V, Fig. 2) can be assigned to the genus *Graphoceras* and belong to the Concavum Subzone of the Concavum Zone, because typical fossils for the Formosum Subzone as *Eudmetoceras* sp. only occur in the layer above. The habitus of the Graphoceratides tends to the older forms. We also found bivalves and belemnites in this layer.

Layer 47 is a grey-brown to reddish marl with intraclasts. Numerous skeletal remains, presumably of crinoids, are present. The only ammonite that very likely comes from this layer is a *Eudmetoceras* sp. (Plate V, Fig. 3). We assign, therefore, this layer to the Formosum Subzone of the Concavum Zone.

Layer 48a is an iron-ooid bearing, grey-brown claystone. The content of iron ooids decreases upwards in comparison with Layer 47. This layer contains only a few fossils (crinoids, belemnites, ammonites), including some incomplete specimens of *Graphoceras* sp. (not figured).

Layer 48b is very similar to the previous layer, but contains local iron-ooid bearing, calcareous concretions. Fossils are very common in this layer: the belemnite *Holcobelus blainvillei* (VOLTZ 1830) is most conspicuous (see also Plate V, Fig. 8). Ammonites are rare, *Hyperlioceras* sp. (not shown) is present as several incomplete specimens. Remarkable is a rhyntonellid that we identify as *Homoeorhynchia* cf. *meridionalis* (EUDES-DESLONGCHAMPS 1863) (Plate V, Fig. 1a, b). In addition, spines of a *Caenocidaris* species occur (Plate V, Fig. 5), which are similar to *Caenocidaris pacomei* (COTTEAU 1884), but have a more rounded shaft than the latter species. Bivalves are relatively common: *Mytilus* sp., *Inoperna sowerbyana* (D'ORBIGNY 1847) (see also Plate V, Fig. 7), *Chlamys textoria* (SCHLOTHEIM 1820), a *Pholadomya* species, and *Pleuromya* sp. also occur. Rarely occur also small, unspecified calcareous sponges (Plate V, Fig. 6).

Layer 48c is almost identical to 48b, but has no intraclasts. The number of iron ooids decreases upwards. We could recover *Sonninia* (*Euhoploceras*) *marginata* (BUCKMANN 1892) (Plate V, Fig. 10) and some juvenile *Hyperlioceras* (not shown) from this layer. Furthermore, bivalves of the species *Pleuromya alduini* (BRONGNIART 1821) and of the genus *Nucula* and a shark

tooth of the genus *Sphenodus* were found. The remaining fauna corresponds to that of Layer 48b.

Layer 49a is a dark grey, silty claystone with light grey to light bluish grey thin sandy lenses (Fig. 9). No fossils could be found here.

Layer 49b has the same lithology as Layer 49a, but contains single shells of a *Gryphaea* species and *Holcobelus blainvillei* (VOLTZ 1830).

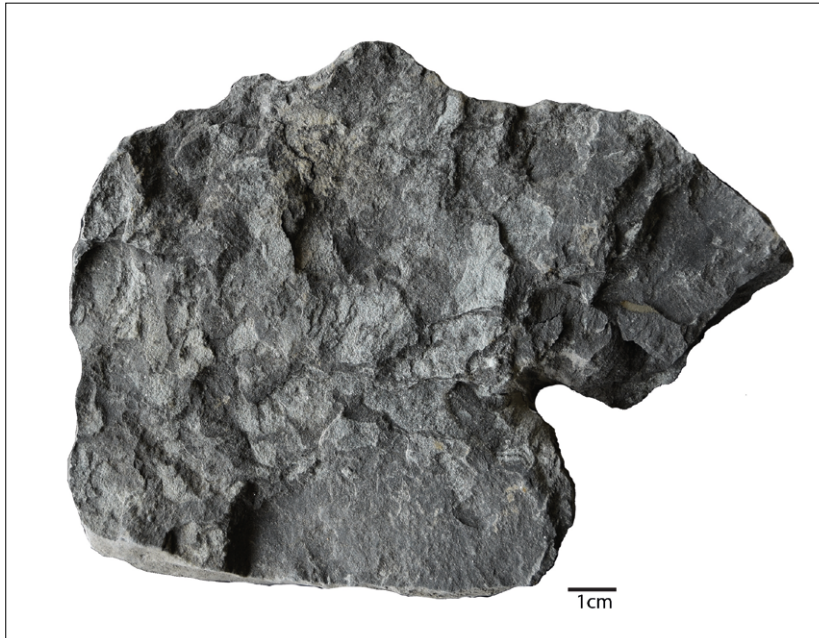


Figure 9: Silty claystone with light grey to lightbluish grey sandy lenses, rock sample from Layer 49a (NMBE 5035819).

2.1.6 Niche Passwang

The Passwang Formation was excavated in Niche Passwang (for location and section see Figs. 1 and 10) in very short time. However, the final tunnel face and 5 geological windows are preserved and permanently accessible. Since the niche lies perpendicular to the stratification, the thickness of the corresponding section is probably accurate since it did not have to be estimated, in contrast to the obliquely cut layers in Ga18/Niche P3.

The two sections (Ga18/Niche P3 and Niche Passwang; see Fig. 10) allow lateral lithological changes to be studied at a relatively short distance (ca. 150 m).

In this context, we note that the section Ga18/Niche P3 could be investigated over a much longer time period. This allowed us to investigate various subsections that were ultimately combined to form an overall section (see Fig. 5). In contrast, the section of Niche Passwang was completed in just 3 working days. Thus, only slightly over 30 min were available to record the section during the mapping. Accordingly, the lithological interpretation is imprecise here. The greatest difference in the sequence studied between Ga18/Niche P3 and Niche Passwang lies in the number of fossils we could recover due to the oblique excavation of the layers in Niche P3 (perpendicular in Niche Passwang). Since the excavation of the layers in Ga18/Niche P3 covered a longer period of time, more fossils could

be collected than in Niche Passwang. Correlation of the two sections in the lower part of the upper Sissach Member was correspondingly difficult (Niche P3: Layers 30–43, Niche Passwang: Layers 29–42, Fig. 10). The upper part was more easily correlatable due to the very similar lithology and partially corresponding fossil content.

Only two ammonites were found in Niche Passwang: in Layer 33 an *Ancolioceras* sp. This indicates probably the Murchisonae Zone, Haugi Subzone. In Layer 46a a *Brasilia* sp. indicates the Bradfordensis Zone, Gigantea Subzone.

2.2 Comparison with the BDB-1 drill core

The BDB-1 drill cut through the entire rock strata exposed during construction of Ga18 and excavation of the associated niches. Although the drill core was recovered and recorded as accurately as possible, many more details could be observed and documented in the sections recorded during construction of Ga18/Niche P3 and Niche Passwang (Fig. 11) than in the drill core of the BDB-1 itself (REISDORF et al. 2016, HOSTETTLER et al. 2017).

In Ga18 (including niches), the individual rock layers were much more extensively exposed, allowing a better overview. In particular, our knowledge of the fossils from individual layers could be significantly improved by collecting in the laboratory and especially from the piles of excavated material. As a result, the ammonite stratigraphy could also be considerably refined compared to that recovered from the BDB-1 well. The main results are summarised below.

- (1) Thickness of the calcareous and iron-oolithic section in the upper part of the Sissach Member (Fig. 10) in the BDB-1 well is 7.5 m, thus significantly larger than in Ga18/Niche P3 (approx. 4.25 m) and Niche Passwang (approx. 4.7 m). The lower part of the Sissach Member seems to have a constant thickness of about 3.5 m. In the area of alternating sandy limestone and silty claystones in the lower part of the upper Sissach Member, a clear correlation between the two sections and the BDB drillcore does not seem possible. In contrast, due to the lithology and the fossil content, the upper iron-oolithic beds can be well correlated. If we compare the two sections with the surface section at Sous les Roches (Fig. 11), this results in a different correlation than that suggested by REISDORF et al. (2016, Fig. 4–1). It is not possible to correlate Layers 11–21 in the Sous les Roches section with Layer 29 in the Niche P3 section and Ga18 (Fig. 5 and Fig. 11 this paper) because the lowest layer of the Sissach Member is not exposed in the Sous les Roches section.

For the corresponding section in the upper part of the Sissach Member and the lower iron-oid bearing part of the Passwang Formation (not subdivided in the study area by REISDORF et al. 2016 or HOSTETTLER et al. 2017), this would result in a small increase in thickness from the Sous les Roches surface section (REISDORF et al. 2016, HOSTETTLER et al. 2017) (thickness approx. 4.5 m) to that of Ga18/Niche 5 (thickness approx. 4.7 m) and to that of the BDB-1 well (drillcore length 7.5 m). The low value of the thickness of the upper part of the Sissach Member (4.25 m) of Ga18/Niche 1 can be the result of imprecision in measuring the angular section of the layers.

- (2) Excavation of Ga18/Niche P3 yielded a significant improvement, especially for the ammonite stratigraphy (see Table 1).

Table 1: Comparison of the results of the ammonite stratigraphy of the Opalinus Clay, the Sissach Member and the overlying lowermost iron-oooid bearing part of the Passwang Formation of the BDB-1 well (not subdivided in the study area) with those of Ga18/Niche P3.

		Zone	Subzone
Bajocian	early	Discites	
	late	Concavum	Formosum
	Concavum		
Aalenian	middle	Bradfordensis	Giganteus
			Bradfordensis
	Murchisonae	Murchisonae	
		Haugi	
	early	Opalinum	«Comptum»
			Opalinum

BDB-1 borehole (REISDORF et al. 2016, HOSTETTLER et al. 2017)

		Zone	Subzone
Bajocian	early	Discites	
	late	Concavum	Formosum
	Concavum		
Aalenian	middle	Bradfordensis	Giganteus
			Bradfordensis
	Murchisonae	Murchisonae	
		Haugi	
early	Opalinum	«Comptum»	
	Opalinum	Opalinum	

Ga18 / Niche 1 (this study)

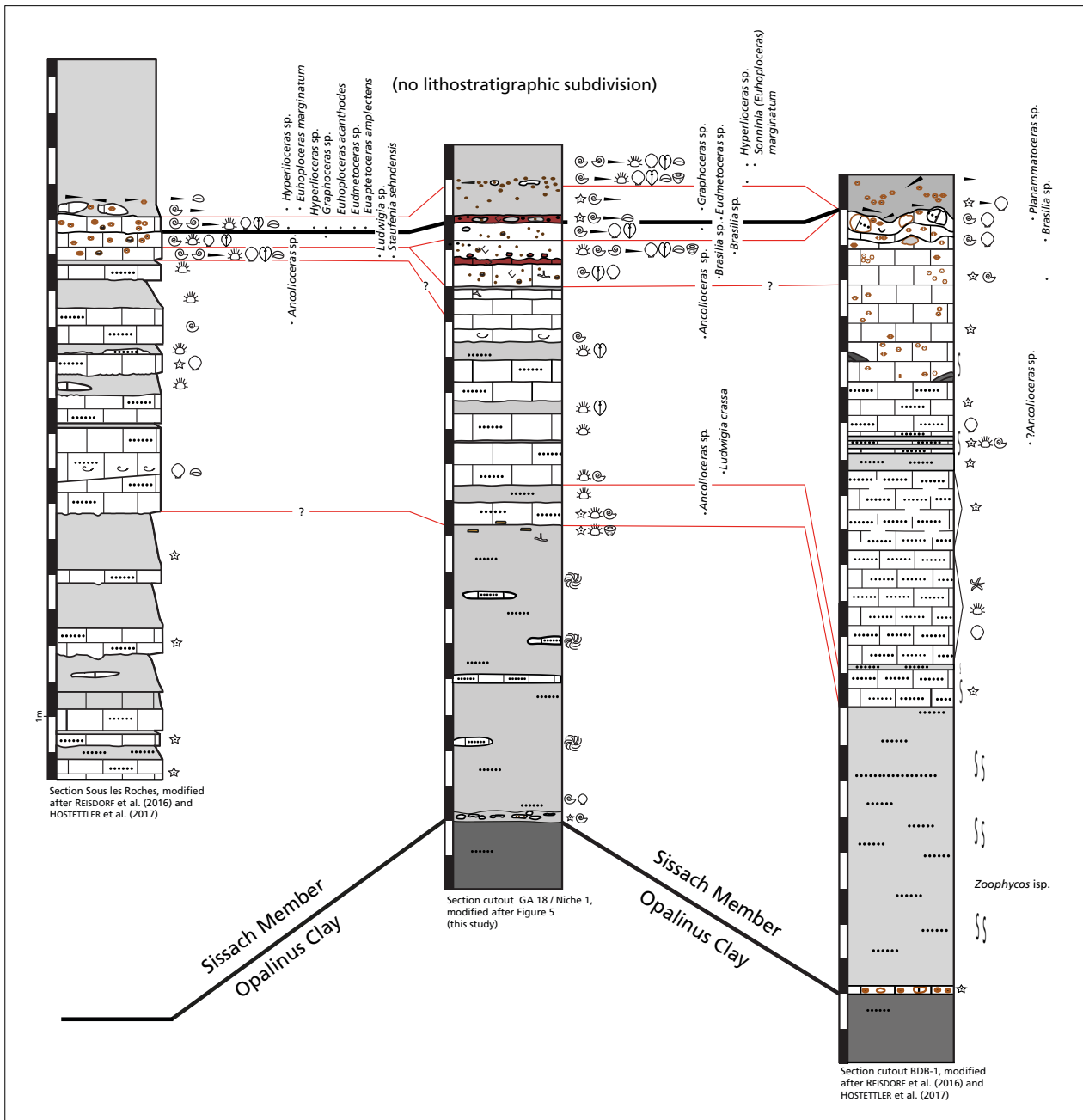


Figure 11: Possible lithostratigraphic correlation of the sections Sous les Roches, Ga18/Niche P3 (Mont Terri Rock Laboratory) and BDB-1 well (Mont Terri Rock Laboratory).

3. Discussion

The biostratigraphical investigations have led to a significantly improved ammonite stratigraphy in the Opalinus Clay and the deepest part of the Passwang Formation in the Mont Terri Rock Laboratory. While in the BDB-1 drillhole only the Opalinum and the Bradfordensis Zone could be clearly assigned with ammonites (Table 1, left part: observed zones and subzones are highlighted in grey), now all ammonite zones and subzones could be assigned with the exception of the Murchisonae Subzone (see Table 1, right part: observed zones and subzones are highlighted in grey).

At the southern edge of the Delémont Basin, the uppermost Opalinus Clay, the Sissach, the Hauenstein and Hirnichopf Member show the least thickness in the region (see also BURKHALTER 1996). The total thickness of these units, condensed there, at Hautes-Roches BE and Creux de la Gélina JU is estimated to be only ca. 1 m. One of the authors (BERNHARD HOSTETTLER) was able to determine this on several blocks in stream beds. The base is an often preserved relict iron oolite, which contains ammonites from the *lineatum* horizon (Opalinum Subzone, Opalinum Zone). Overlying this layer is also an iron oolitic layer with numerous reworked clasts from the Opalinus Clay. This layer probably corresponds to layer 28 (Fig. 5) in the Mont Terri Rock Laboratory, which is also called basal hard-ground. According to Burkhalter (1996), this bed was deposited in the «Comptum» Subzone of the Opalinus Zone. We found no usable ammonites from this layer in the Mont Terri Rock Laboratory.

Above this, at Les Hautes Roches BE, an iron oolite follows that is practically without any fossils. Only in the uppermost part does it contain numerous fossils: ammonites of the genus *Graphoceras* and rostra of *Holcolobus blainvillei* (VOLZ 1830) become frequent. Based on ammonite findings, this section corresponds to the «condensed equivalent» of the Hauenstein Member (according to BURKHALTER 1996). This layer correlates with Layer 46b in Fig. 5. In the 10 cm above, *Euaptetoceras amplexens* (BUCKMAN 1889) and *Eudmetoceras* sp. are common along (indicating the Formosum Subzone) with belemnite rostra. This section probably correlates with Layer 47 (Fig. 5) in the Mont Terri Rock Laboratory. Above follows a location with Euhoplocerates (especially *E. acanthodes* (BUCKMAN 1889) and still a little higher, a layer with *Hyperliocerates* (indicating the Discites Zone) forms the conclusion of this sequence. This area can be correlated with Layers 48a–c in the Mont Terri Rock Laboratory. Based on their allocation, the Layers 47–48c (Fig. 5) in the Mont Terri Rock Laboratory probably correspond to the Late Concavum to Discites Zones and to the condensed equivalent of the Hirnichopf Member sensu BURKHALTER (1996). In a landslide of the Opalinus Clay to the W of Les Vieux Ponts, S Châtillon JU (south of Delémont), one of the authors (BERNHARD HOSTETTLER) found the same sequence in blocks. This means that this condensed sequence in the Passwang Formation reaches all the way to the southern edge of the Delémont Basin.

In the Mont Terri Rock Laboratory, a sequence of sandy marls, calcareous sand lenses and banks follows the reworked horizon at the base of Sissach Member. These deposits (Layers 29a–b in Fig. 5) are strongly

bioturbated. Characteristic is the occurrence of the trace fossil *Zoophycos* isp. This sequence corresponds to the lower parasequence as described by BURKHALTER (1996) in the north of the Delémont Basin. The few ammonite finds in the Mont Terri Rock Laboratory show that these deposits were formed during the «Comptum» Zone. The middle section of the Sissach Member (Fig. 5, Layers 30–43) in the Mont Terri Rock Laboratory has a thickness of slightly less than 3.5 m. It consists of sandy limestone, sandy claystones and above, biotrititic limestones. Compared to the southern Delémont Basin, this area is not condensed. The few ammonites indicate deposition mainly in the Murchisonae Zone. As indicated by increased deposition of limonitised components and iron ooids, the youngest section of the Sissach Member in Mont Terri is increasingly condensed. Accordingly, the occurrence of fossils increases upwards. We subdivided Layer 46 into a lower part (a) and an upper part (b) solely on the basis of the fossils: while the lower part (a) contains ammonites from the Giganteum Subzone of the Bradfordensis Zone, the upper part (b) contains ammonites from the earlier Concavum Zone. Lithologically this bank cannot be meaningfully subdivided. Therefore, like the corresponding bed (depth 97.8–95.5 m) in the BDB 1 borehole (see REISDORF et al. 2016, HOSTETTLER et al. 2017), it is here placed in the Sissach Member, contrary to the definition of LIEB (1953) and BURKHALTER (1996).

In the area of the landslide near Le Champois, to the E of Soubey JU, we found the following profile: over a 3 m-thick sequence of thick-bedded biotrititic limestones with few fossils lies an iron-oolite bearing fossil-rich horizon. Ammonites from the Bradfordensis Zone, Gigantea Subzone, and from the earlier Concavum Zone are abundant. This sequence probably corresponds to Layer 46 (Fig. 5) in the Mont Terri Rock Laboratory. Above another layer of biotrititic limestone of unknown thickness, a clayey layer with iron ooids was found locally in the landslide. It frequently contained *Holcobelus blainvillei* (VOLTZ 1830) and *Homoeorhynchia* cf. *meridionalis* (EUDES-DESLONGCHAMPS 1863). Ammonites could not be found. Due to the fossils recorded here, this sequence can best be correlated with the Layers 48a–c (Fig. 5) in the Mont Terri Rock Laboratory. This indicates very probably Concavum Zone, Formosum Subzone to Discites Zone and thus corresponds to the condensed equivalent of the Hirnichopf Member of BURKHALTER (1996).

4. Conclusions

Although, with few exceptions, the fossil material could not be recovered in outcrop with exception of the tunnel face in Ga18/Niche Passwang, the majority of the fossils could be assigned to their corresponding layers using the lithological peculiarities of the different rock strata.

Due to the extension of the Mont Terri Rock Laboratory (Ga18) and the ammonites that we found in the excavated material, we could significantly improve the biostratigraphic dating of the Sissach Member and the overlying lowermost iron-oid bearing part of the Passwang Formation. With the exception of the Murchisonae Subzone, all ammonite standard Zones and Subzones from Early Aalenian to Earliest Bajocian are found.

Comparison of the new profiles recorded in the Rock Laboratory with those of Sous les Roches and those of the BDB-1 borehole enabled us to make a new correlation, especially those of Sous Les Roches profile with the new profiles (Fig.11). This additional information also allowed us to better correlate the new profiles with outcrops in the S and N of the Delémont Basin and further southwest at Soubey JU. The thickness of the sequence of Sissach to the probably condensed equivalent of the Hirnichopf Member increases from about 1 m at the southern edge of the Delémont Basin to almost 9 m in the Mont Terri Rock Laboratory. This increase in thickness could possibly be explained by differential subsidence (see also BURKHALTER 1996).

References

- BRONGNIART, A. (1821): Sur les caractères zoologiques des formations, avec l'application de ces caractères à la détermination de quelques terrains de Craie. – *Ann. Mines* 6, 537–572.
- BURKHALTER, R. M. (1996): Die Passwang-Alloformation (unteres Aalénien bis unteres Bajocien) im zentralen und nördlichen Schweizer Jura. – *Eclogae geol. Helv.* 89/3, 875–934.
- BUCKMAN, S. S. (1887–1907): A monograph of the ammonites of the “Inferior Oolite Series” (Stages – Toarcian, Pars; Aalenian; Bajocian; Bathonian, Pars). Vol. I. Atlas. – *Monogr. palaeontogr. Soc. (London)*, 61/292.
- CONTINI, D., ELMI S., MOUTERDE, R. & RIOULT M. (1997): Aalénien. In: Cariou, E. & P. Hantzpergue (Ed.): *Biostratigraphie du Jurassique ouest-européen et méditerranéen: zonations parallèles et distribution des invertébrées et microfossiles* (p.37–40). – *Bull. Cent. Rech. Elf Aquitaine Explor. – Prod.* 17.
- COTTEAU, G. (1884): Echinides réguliers. Familles des Cidaridés et des Salénidés. Tome 10, première partie. In: *Paléontologie française*. – Masson, Paris.
- WANCE, J. M. L. (1825): In H. M. D. de Blainville (Éd.): *Manuel de malacologie et de conchyliologie*. – Levrault, Strasbourg.
- DESOR, E. (1858): Synopsis des échinides fossiles. – Kreidel & Niedner, Wiesbaden.
- DIETZE, V., RIEBER, H., AUER, W., FRANZ, M., SCHWEIGERT, G., CHANDLER, R. B., RIETER, M. & CHIARINI, R. (2014): Aalenian (Middle Jurassic) ammonites and stratigraphy of the Geisingen clay pit (SW Germany). – *Palaeodiversity* 7, 61–127.
- DUMORTIER, E. (1864–1875): Dépôts jurassiques du Bassin du Rhone. Quatrième partie: Lias supérieur. – F. Savoy, Paris.
- EDES-DESLONGCHAMPS, E. (1862–1885): *Paléontologie française. Terrains jurassiques 6: Brachiopodes*. – Masson, Paris.
- HEER, O. (1865): *Die Urwelt der Schweiz*. – Schulthess, Zürich.
- HORN, E. (1909): Die Harpoceraten der Murchisonae-Schichten des Donau-Rhein-Zuges. – *Mitt. bad. geol. Landesanst.* 4/1, 251–323.
- HOSTETTLER, B., REISDORF, A. G., JAEGGI, D., DEPLAZES, G., BLAESI, H. MORARD, A., FEIST-BURKHART, S. WALTSCHEW, A., DIETZE, V. & MENKVELD-GFELLER, U. (2017): Litho- and biostratigraphy of the Opalinus Clay and bounding formations in the Mont Terri rock laboratory (Switzerland). – *Swiss J. Geosci.* 110/1, 23–37.
- JAEGGI, D., GALLETI, M., AMACHER, F., DUNST, R., NUSSBAUM, C., RASELLI, R., RINGEISEN, M., SCHEFER, S. & BOSSART, P. (2020): Gallery 2018: Excavation and geological documentation. – Mont Terri tech. Rep. TR2018-04.
- LIEB, F. (1953): Neue Beiträge zur Erforschung der Ammonitenhorizonte der Murchisonae-Schichten des schweizerischen Juragebirges. – *Eclogae geol. Helv.* 46, 286–294.
- MASSALONGO, A. (1855): *Zoophycos, novum genus Plantarum fossilium*. – *Monographia – Typis Antonellianis, Veronae*.
- OPPEL, A. (1856): Die Juraformation Englands, Frankreichs und des südwestlichen Deutschlands. – *Württemb. natw. Jh.* 12, 121–556.
- ORBIGNY, A. D' (1842–1851): *Paléontologie française. Terrains jurassiques. I. Cephalopodes*. – Masson, Paris.
- REINECKE, J. C. M. (1818): *Maris protogaei Nautilus et Argonautae vulga Cornua Ammonis in Agro Coburgico et vicinio reperiundos; descripsit et delineavit, simul Observationes de Fossilium Protypis*. – L. C. A. Ahlhi imp., Coburg.
- REISDORF, A. G., HOSTETTLER, B., JAEGGI, D., DEPLAZES, G., BLAESI, H., MORARD, A., FEIST-BURKHARDT, S., WALTSCHEW, A., DIETZE, V. & MENKVELD-GFELLER, U. (2016): Litho- and biostratigraphy of the 250 m-deep Mont Terri BDB borhole through the Opalinus Clay and bounding formations, St-Ursanne Switzerland. – Mont Terri tech. Rep. TR2016-02.
- REISDORF, A. G., HOSTETTLER, B., WALTSCHEW, A., JAEGGI, D. & MENKVELD-GFELLER, U. (2014): Biostratigraphy of the basal part of the Opalinus-Ton at the Mont Terri rock laboratory, Switzerland. – Mont Terri tech. Rep. TR2014-07.
- ROEMER, F. A. (1836): *Die Versteinerungen des Norddeutschen Oolithen-Gebirges*. – Hahn, Hannover.

- SCHLOTHEIM, E. F. VON (1820–1823): Die Petrefactenkunde auf ihrem jetzigen Standpunkte durch die Beschreibung seiner Sammlung versteinierter und fossiler Überreste des Thier und Pflanzenreichs der Vorwelt erläutert. – Becker, Gotha.
- SEIFERT, I. (1963): Die Brachiopoden des Oberen Dogger der Schwäbischen Alb. – *Palaeontographica (A)* 121/4–6, 156–203.
- SOWERBY, J. (1812–1846): The mineral conchology of Great Britain; or, coloured figures and descriptions of those remains of testaceous animals or shells, which have been preserved at various times and depths in the earth (vol. 1–7). – Meredith, London.
- VADET, A. (1991): Révision des «Cidaris» du Lias et du Dogger européens. – *Mém. Soc. Acad. Boulonnais* 10, 1–191.
- VOLTZ, P. L. (1830): Observations sur les bélemnites. – *Mém. Soc. Hist. nat. Strasbourg* 1, I–IV.

Acknowledgements

We thank our colleagues from the Mont Terri Rock Laboratory, in particular Raeto Raselli and Senecio Schefer for their support with the fieldwork. For reviewing the report in detail we are grateful to Gaudenz Deplazes from Nagra; his helpful comments lead to an improvement of the content. We furthermore thank Regina Hostettler for her precious support in searching and collecting the fossils from the tailings. Finally we thank Roy W. Freeman for improving the English of this report.

Appendix

Plates I–V, p. 30–39

Description of the geological windows, p. 40–41

Plate I

- Fig. 1 *Leioceras subglabrum* (BUCKMAN 1902), NMBE 5035763. Flattened macroconch with partially preserved shell. Ga18/Niche CO₂, lower shaly facies.
- Fig. 2 *Leioceras subglabrum* (BUCKMAN 1902), NMBE 5035764. Macroconch; body chamber filled with sediment. Ga18/Niche CO₂, lower shaly facies.
- Fig. 3 Top right: *Leioceras subglabrum* (BUCKMAN 1902), 5035766. Flattened microconch. Bottom left: *Cylicoceras* sp., NMBE 5035767. All with shell preservation. Ga18/Niche CO₂, lower shaly facies.
- Fig. 4 4a: Band-shaped agglomeration of the mussel *Bositra buchi* (ROEMER 1836), NMBE 5035768. Ga18, upper sandy facies.
4b: Enlarged detail from 4a.
- Fig. 5 ?*Leioceras* sp., NMBE 5035769. Ga18/Niche CO₂, lower sandy facies.
- Fig. 6 *Meleagrinnella* sp., NMBE 5035773. Ga18/Niche CO₂, lower carbonate-rich sandy facies
- Fig. 7 *Palaeonucula hammeri* (DEFRANCE 1825), NMBE 5035770. Ga18/Niche CO₂, lower shaly facies.
- Fig. 8 *Costatrchus subduplicatus* var. *palinurus* (D'ORBIGNY 1850), NMBE 5035771. Ga18/Niche CO₂, lower shaly facies.
- Fig. 9 *Nuculana claviformis* (SOWERBY 1824), NMBE 5035772. Ga18/Niche CO₂, lower shaly facies.
- Fig. 10 Echinid spine, NMBE 5035773. Ga18/Niche CO₂, carbonate-rich sandy facies.
- Fig. 11 Detail of a carbonate-rich layer with unidentified oysters (2), crinoid stem fragments (*Chariocrinus wuerttembergicus* OPPEL 1856) (1) and an interambulacral plate of an echinid (*Cidaroidea* indet.) (3), NMBE 5035773. Ga18, upper sandy facies.
- Fig. 12 *Leioceras* ex gr. *opalinum* (REINECKE 1818), NMBE 5035774. Ga18, upper sandy facies.



1



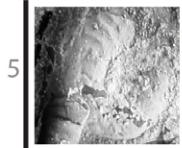
2



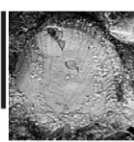
3



12



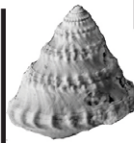
5



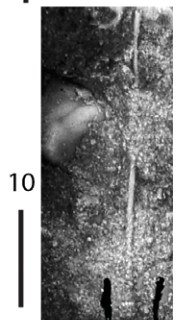
6



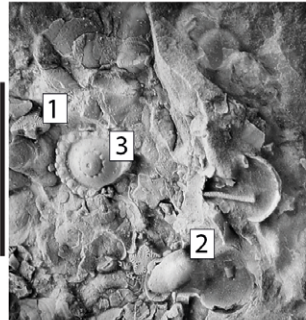
7



8



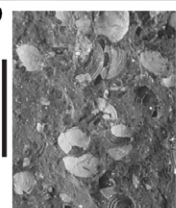
10



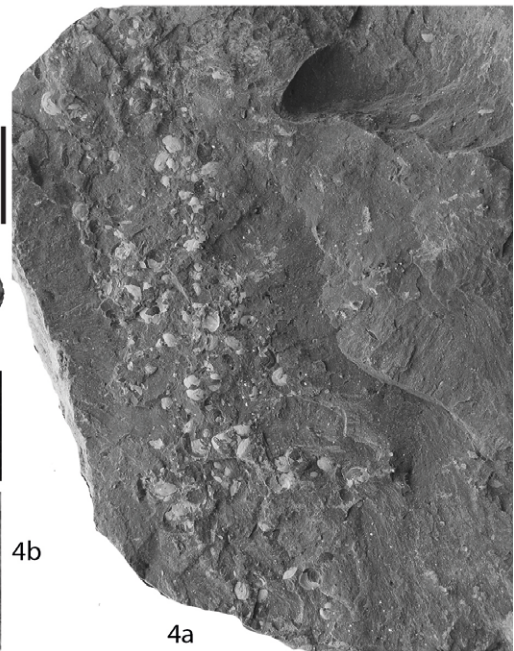
11



9



4b

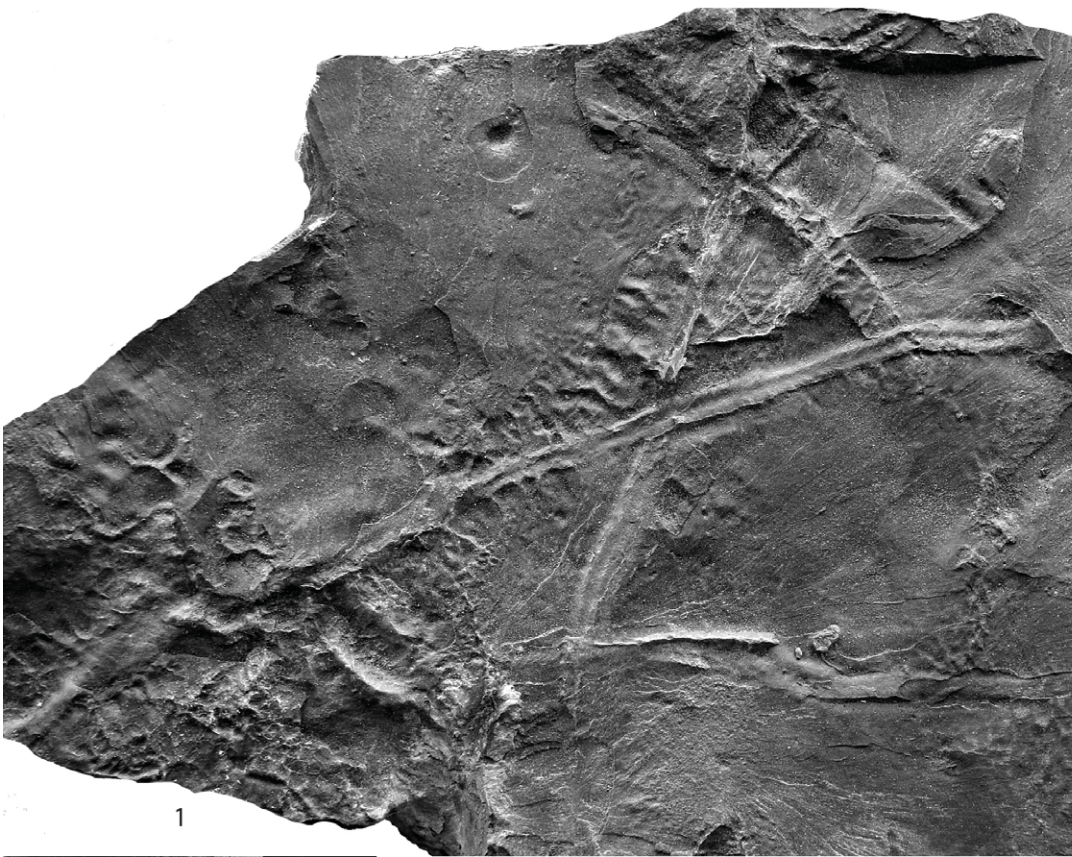


4a

1cm

Plate II

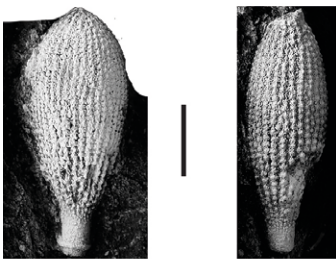
- Fig. 1 *Gyrochorte* isp., NMBE 5035775. Ga18, Opalinus Clay, upper sandy facies.
- Fig. 2 *Leioceras* ex gr. "*comptum*", NMBE 5035777. Ga18, Sissach Member, Layer 29a.
- Fig. 3 ?*Ancolicer* nov. sp., NMBE 5035778. Ga18, Sissach Member, Layer 31.
- Fig. 4 ?*Ancolicer* nov. sp., NMBE 5035779. Ga18, Sissach Member Layer 31.
- Fig. 5 *Caenocidaris royssii* (DESOR 1858), NMBE 5032524. Ga18/Niche P3, Sissach Member, Layer 30.
- Fig. 6 *Caenocidaris royssii* (DESOR 1858), NMBE 5032525. Ga18/Niche P3, Sissach Member, Layer 30.
- Fig. 7 *Caenocidaris royssii* (DESOR 1858), NMBE 5032523. Ga18/Niche P3, Sissach Member, Layer 32.
- Fig. 8 *Pholadomya* sp., NMBE 5035780. Sissach Member.
- Fig. 9a, b Vertebra of a Plesiosaur, NMBE 5935781. Ga18, Sissach Member, Layers 33–37.



1



2



5

6



3



4



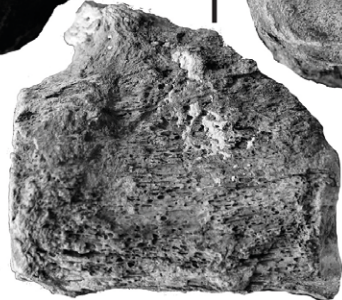
9a



7



8

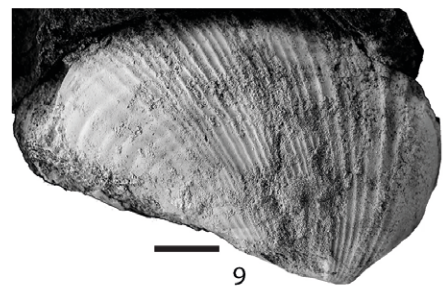
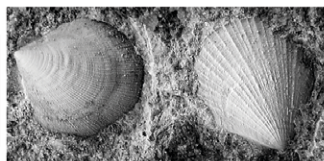
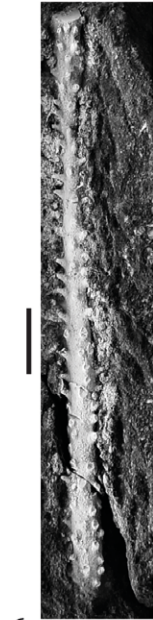
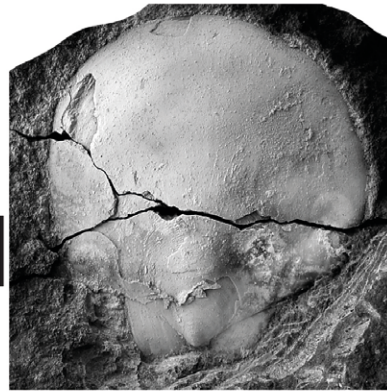
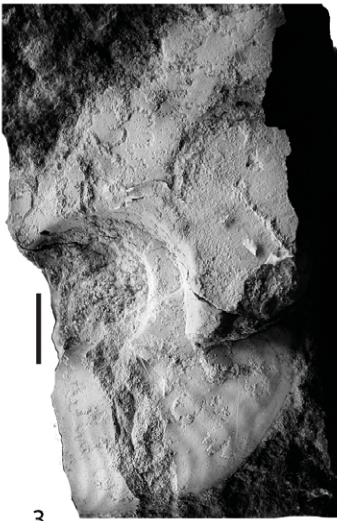


9b

1cm

Plate III

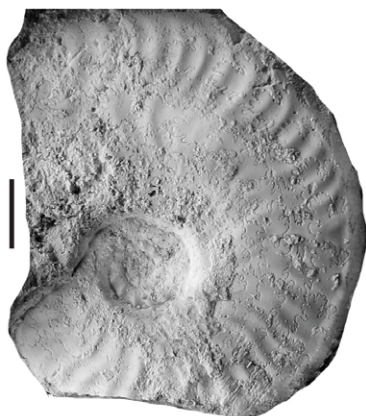
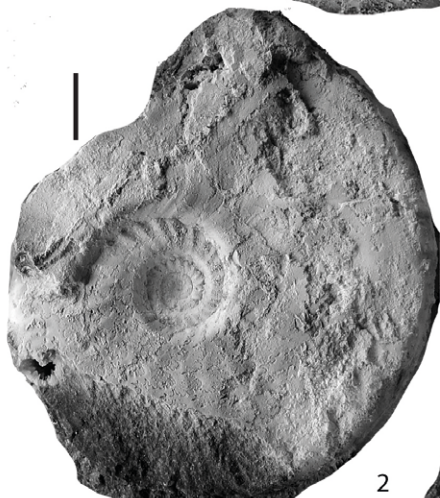
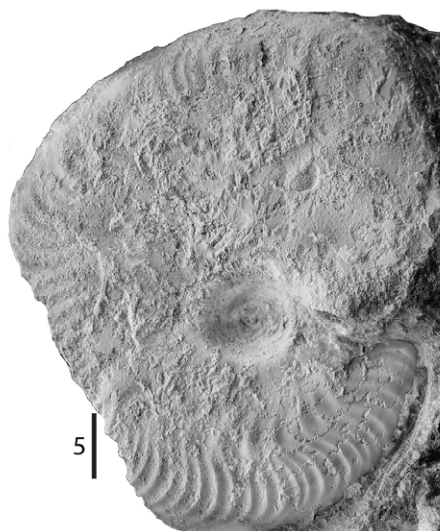
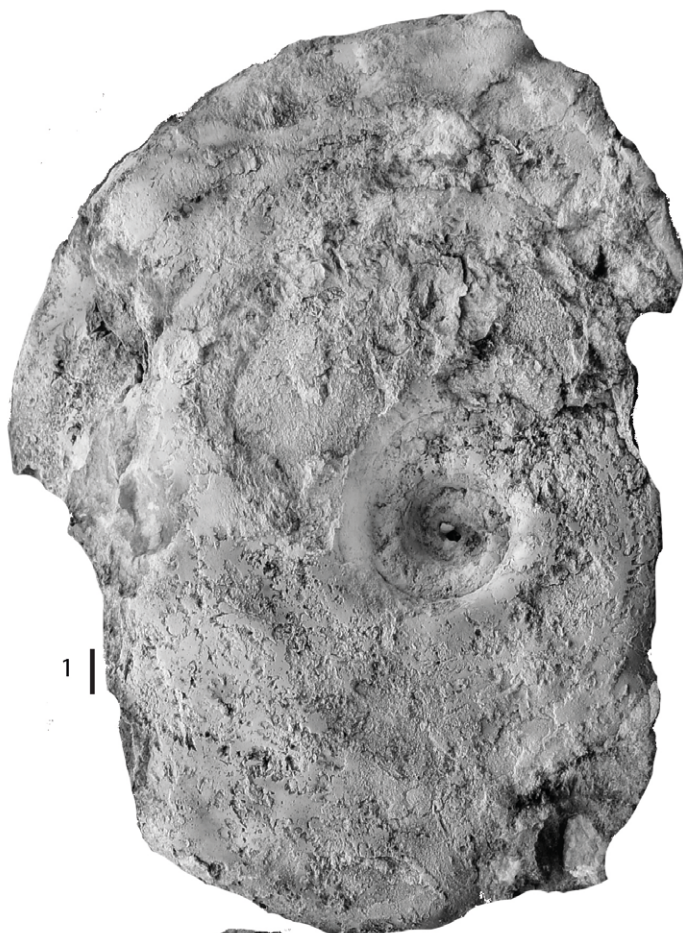
- Fig. 1 *Ludwigia crassa* HORN 1909, NMBE 5035782. Ga18, Sissach Member, Basis Layer 33.
- Fig. 2 *Brevibelus breviformis* (VOLTZ 1830), NMBE 5035783. Ga18, Sissach Member, Basis Layer 33.
- Fig. 3 *Ancolloceras* sp., NMBE 5035786. Ga18, Sissach Member, Layer 39.
- Fig. 4 *Goniomya literata* (SOWERBY 1819), NMBE 5035787. Ga18, Sissach Member, Layers 33–37.
- Fig. 5 *Entolium* sp., NMBE 5035788. Ga18, Sissach Member, Layer 31.
- Fig. 6 Primary spine of *Diplocidaris* sp., NMBE 5035760. Ga18/Niche P3, Sissach Member, Layer 38.
- Fig. 7 *Gigantothyris* cf. *gigantea* (SEIFERT 1963), NMBE 5035789. Ga18, Sissach Member, Layer 46a.
- Fig. 8 *Propeamussium* sp., NMBE 5035790. Ga18, Sissach Member, Layer 39.
- Fig. 9 *Pholadomya fidicula* (SOWERBY 1826), NMBE 5035792. Ga18, Sissach Member, basis Layer 33.
- Fig. 10 *Brasilia* sp., NMBE 5035793. Ga18, Sissach Member, Layer 44.



1cm

Plate IV

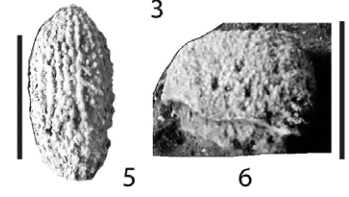
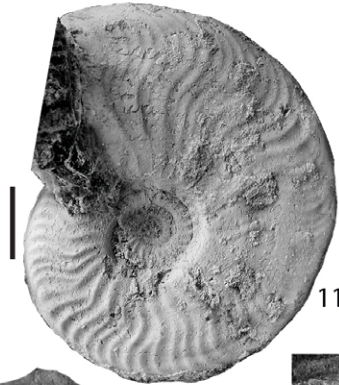
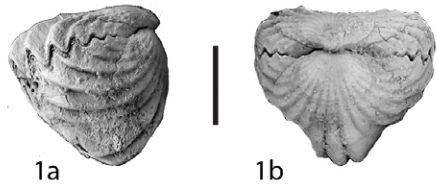
- Fig. 1 *Brasilia* sp., NMBE 5035794. Ga18, Sissach Member, Layer 46a.
Fig. 2 *Brasilia* sp., NMBE 5035795. Ga18, Sissach Member, Layer 46a.
Fig. 3 *Brasilia* sp. microconch, NMBE 5035796. Ga18, Sissach Member, Layer 46a.
Fig. 4 *Brasilia* sp., NMBE 5035797. Ga18, Sissach Member, Layer 46a.
Fig. 5 *Graphoceras* sp., NMBE 5035798. Ga18, Sissach Member, Layer 46b.
Fig. 6 *Graphoceras* sp., NMBE 5035799. Ga18, Sissach Member, Layer 46b.
Fig. 7 *Graphoceras* sp., NMBE 5035800. Ga18, Sissach Member, Layer 46b.



1cm

Plate V

- Fig. 1a, b *Homoeorhynchia* cf. *meridionalis* (EUDES-DESLONGCHAMPS 1863), NMBE 5035801. Ga18, Passwang Formation.
- Fig. 2 *Graphoceras* sp., NMBE 5035803. Ga18, Sissach Member, Top Layer 46b.
- Fig. 3 *Eudmetoceras* sp., NMBE 5035804. Ga18, Sissach Member, Layer 47.
- Fig. 4 *Chlamys textoria* (SCHLOTHEIM 1820), NMBE 5035805. Ga18, Sissach Member, Layer 48c.
- Fig. 5 *Caenocidaris* cf. *pacomei* (COTTEAU 1884), NMBE 5035806. Ga18, Sissach Member, Layer 46.
- Fig. 6 Calcareous sponge, NMBE 5035807. Ga18, Sissach Member, Layer 48c.
- Fig. 7 *Inoperna sowerbyana* (D'ORBIGNY 1847), NMBE 5035808. Ga18, Sissach Member, Layer 48b.
- Fig. 8 *Holcobelus blainvillei* (VOLTZ 1830), NMBE 5035809. Ga18, Sissach Member, Layer 48c.
- Fig. 9 *Ctenostreon* sp., NMBE 5035812. Ga18, Sissach Member, Layer 46a.
- Fig. 10 *Sonninia* (*Euhoploceras*) *marginata* (BUCKMAN 1892), NMBE 5035813. Ga18, Sissach Member, Layer 48c.
- Fig. 11 *Brasilia* sp., NMBE 5035814. Ga18, Sissach Member, Layer 46a.



1cm

DESCRIPTION OF THE GEOLOGICAL WINDOWS IN THE MONT TERRI ROCK LABORATORY, GALLERY 18 (GA18)

Geological windows have been placed at the most important places so that the various lithologies in the Mont Terri Rock Laboratory, which are otherwise covered with shotcrete, remain visible. These provide direct access to the different lithological units and their facies. For the location of windows and sections in Ga18 please see Fig. 2.

Niche P3

Window 1 (F1 in Fig. 2): visible are brown limestones with iron ooids and limonitised components. The fossil content consists of echinoderm skeletal elements, shells, and bryozoans. Up to 10 cm-wide open-solution enlarged fractures partially with coatings of residual clays are visible and fissure edges are covered with calcite crystals. The solution-enlarged fractures seem to be related to a rather young and very local karst phenomena featuring advective flow in this part of the Passwang Formation (JAEGGI et al. 2020). The position of these fractures is well above the top Sissach Member in the depth range of 85 to 90 m at BDB-1 (REISDORF et al. 2016).

Ga18

- Window 2 (F2): here the marls of Layer 49 (Fig. 5) are exposed.
- Window 3 (F3): here the Layers 45–48 are visible (see Fig. 5). The transition from the Sissach Member (Passwang Formation) to the undifferentiated Passwang Formation is exposed here in particular.
- Window 4 (F4): visible are the layers (from bottom left to top right) top of Layer 29 to Layer 33 (Fig. 5). In Layer 33 the cross sections of an ammonite and a larger bivalve *Ctenostreon* sp. are visible. In Layer 32 there are several spines of *Caenocidaris royssii* (DESOR 1858). The dark marl under Layer 31 forms the transition to the *Zoophycos* facies of Layer 29.
- Window 5 (F5): this shows the transition from the Opalinus Clay to the Sissach Member of the Passwang Formation (Layers 28, 29a, b, see Fig. 5). In the first layer of Sissach Member there are reworked intraclasts. Above there is the sandier *Zoophycos* facies. Below lies the upper sandy facies of the Opalinus Clay.
- Window 6 (F6): Opalinus Clay, upper sandy facies with calcareous concretions. The larger of the two concretions measures approx. 10 cm in diameter.
- Window 7 (F7): Opalinus Clay with a reddish, calcareous biotrititic section. The biotrititus consists of echinoderm remains and shell detritus.

Niche Passwang

- Window 8 (F8): Opalinus Clay, upper sandy facies. A tectonic overprint is clearly visible that intersects the layers with a steep dip.
- Window 9 (F9): Opalinus Clay upper sandy facies. The steep dip of the layers is clearly visible.
- Window 10 (F10): shows the boundary Opalinus Clay to the Sissach Member of the Passwang Formation. Below the first layer of the Sissach Member, there is a small carbonate concretion with shrinkage cracks. It is filled with calcite at the edges and at one point with ferrous dolomite. The boundary horizon (Layer 28) is well visible

because of its rusty brown color. The *Zoophycos* facies of the Sissach Member follows above (Layer 29a, b, see Fig. 5).

- Window 11 (F11): shows the same facies transition as Window 10.
- Window 12 (F12): Shows the transition from the *Zoophycos* facies to the upper part of the Sissach Member (see Fig. 10, Niche 5: Layers 29–31a). The boundary is marked by the cross section of a sea urchin spine (*Caenocidaris royssii* (DESOR 1858), visible in the lower right corner of the window).
- Tunnel front: the Layers 46b, 47, 48a–c are visible here (see Fig. 10, Niche Passwang). Layer 46 shows cross sections of ammonites among other fossils. Furthermore, a fissure system (analogous to Niche P3) is visible. Layer 48b is very rich in fossils and more carbonate-rich than in Ga18 (bright area in the ceiling).

Niche Fracture

- Window 13 (F13): Opalinus Clay, upper shaly-facies. Dark claystone with brown-grey, slightly rusty, thin oblate concretions up to 3 cm thick (siderite?), faulted.
- Window 14 (F14): As window 13, but without concretions; with thin, rusty streaks in the clay, faulted.

Niche CO₂

- Window 15 (F15): Opalinus Clay, transition of the lower shaly-facies into the carbonate-rich sandy facies, with large pyrite nodules at base of carbonate-rich sandy facies.
- Window 16 (F16): Opalinus Clay, lower shaly facies.
- Window 17 (F17): Opalinus Clay, lower shaly facies with the lower pyrite horizon.